Direct evidence of Parkinson pathology spread from the gastrointestinal tract to the brain in rats.

Holmqvist, Staffan; Chutna, Oldriska; Bousset, Luc; Aldrin-Kirk, Patrick; Li, Wen; Björklund, Tomas; Wang, Zhan-You; Roybon, Laurent; Melki, Ronald; Li, Jia-Yi

Published in:
Acta Neuropathologica

DOI:
10.1007/s00401-014-1343-6

2014

Direct evidence of Parkinson pathology spread from the gastrointestinal tract to the brain in rats.

Staffan Holmqvist [1, 2], Oldriska Chutna[1], Luc Bousset [3], Patrick Aldrin-Kirk [4], Wen Li[1], , Tomas Björklund [4], Zhan-You Wang [5], Laurent Roybon [2], Ronald Melki [3], and Jia-Yi Li [1, 5]

[1] Neural Plasticity and Repair Unit, Wallenberg Neuroscience Center, Department of Experimental Medical Science, Lund University, BMC A10, 22184, Lund, Sweden.

[2] Cell Stem Cell laboratory for CNS Disease Modeling, MultiPark Strategic Research Area and Lund Stem Cell Center, Department of Experimental Medical Science, Lund University, BMC A10, 22184, Lund, Sweden.

[3] Laboratoire d′Enzymologie et de Biochimie Structurale, CNRS, Bâtiment 34, Avenue de la Terrasse, 91190 Gif-sur-Yvette, France

[4] Molecular Neuromodulation Unit, MultiPark Strategic Research Area, Wallenberg Neuroscience Center, Department of Experimental Medical Science, Lund University, BMC A10, 22184, Lund, Sweden

[5] Institute of Neuroscience, College of Life and Health Sciences, Northeastern University, 110819, Shenyang, China.

Concise title:

Spread of Parkinson pathology in rats

Correspondence:

Dr. Jia-Yi Li

Neural Plasticity and Repair Unit, Wallenberg Neuroscience Center, Department of Experimental Medical Science, Lund University, BMC A10, 22184 Lund, Sweden, Email: jia-yi.li@med.lu.se, Phone: +46 46 2220525

Or:

Institute of Neuroscience, College of Life and Health Sciences, Northeastern University, 110819, Shenyang, China. Email: jiayili@mail.neu.edu.cn, Phone: +86-24 24245100

Abstract

The cellular hallmarks of Parkinson's disease (PD) are the loss of nigral dopaminergic neurons and the formation of α-synuclein-enriched Lewy bodies and Lewy neurites in the remaining neurons. Based on the topographic distribution of Lewy bodies established after autopsy of brains from PD patients, Braak and coworkers hypothesized that Lewy pathology primes in the enteric nervous system and spreads to the brain, suggesting an active retrograde transport of α-synuclein (the key protein component in Lewy bodies), via the vagal nerve. This hypothesis however has not been tested experimentally thus far. Here, we use a human PD brain lysate containing different forms of α-synuclein (monomeric, oligomeric and fibrillar), and recombinant α-synuclein in an *in vivo* animal model to test this hypothesis. We demonstrate that α-synuclein present in the human PD brain lysate and distinct recombinant α-synuclein forms are transported via the vagal nerve and reaches the dorsal motor nucleus of the vagus in the brainstem in a time-dependent manner after injection into the intestinal wall. Using live cell imaging in a differentiated neuroblastoma cell line, we determine that both slow and fast components of axonal transport are involved in the transport of aggregated α-synuclein. To our best knowledge, this is the first study providing direct evidence that different α-synuclein forms can propagate from the gut to the brain, and that microtubule-associated transport is involved in the translocation of α-synuclein in neurons.

Keywords

Parkinson's disease, alpha-synuclein, Lewy body, protein aggregation, protein propagation

Introduction

Parkinson's disease (PD) is the most common movement disorder and the second most common neurodegenerative disease after Alzheimer's disease. The neuropathological hallmarks of PD are loss of dopaminergic neurons in the substantia nigra and the presence of cytoplasmic inclusions called Lewy bodies and Lewy neurites in the remaining surviving dopaminergic neurons [25]. A large body of evidence suggests that these neuropathological features are not only restricted to dopaminergic neurons, but are also widely exhibited in non-dopaminergic systems. The progressive spread of the Lewy pathology, which is characterized by α-synuclein immunoreactive inclusions in cell bodies and neuronal processes, marks the core of neuropathological staging in most cases of PD. The topographic distribution of α-synuclein-containing inclusions, first appear in the peripheral nervous system (enteric neurons in the gut), progresses to lower brain regions, such as the dorsal motor nucleus of the vagus (DMV) to the substantia nigra (where the primary lesion of dopaminergic neurons locates in PD), and eventually inclusions can be detected in the cerebral cortex. These findings give rise to the notion that a neurotropic pathogen would penetrate the gut epithelium and enter axons of the enteric neurons in the myenteric plexus (Auerbach's plexus); these neurons control the activity of gut smooth muscles and/or the submucosal plexus (Meissner's plexus), which regulates mucosal secretion and blood flow.

Braak and co-workers hypothesized that this pathogen might spread via retrograde transport to different interconnected brain regions [5, 6, 17]. In Braak's observations, Lewy pathology first manifests in enteric neurons of the gut (stage 1) long before it is present in dopaminergic neurons of the midbrain and PD symptoms are evident (stage 3) [7]. The gap between stages 1 and 3 may take many years. From the periphery, the pathology gains access to the lower brainstem via the vagal nerve and then follows an ascending pathway reaching the substantia nigra and subsequently, the cerebral cortex [28, 40]. Thus, the temporal appearance of Lewy

pathology in PD strongly suggests long-distance trafficking of a pathogen in neurons from peripheral tissues to the brain.

We, and others, have shown that intra-striatal transplants of fetal ventral mesencephalic progenitors in PD patients develop Lewy pathology a decade after transplantation, suggesting transfer of Lewy pathology from the host to the grafted cells [21-23, 29, 30]. Further experimental studies have shown that Lewy pathology can indeed propagate from one cell to another, not only in cultured cells *in vitro*, but also in brains of animal models of PD [11, 15, 27, 33]. Moreover, recent reports revealed that α-synuclein could spread along the projection tracts after it was directly injected into the brain of α-synuclein transgenic or wildtype mice [31, 32, 43]. Lee and colleagues elegantly showed deposition of α-synuclein in myenteric neurons after injecting the brain lysate derived from the patient of dementia with Lewy body (DLB), into the stomach wall of A53T transgenic mice [26], but to date, experimental evidence is lacking to show whether α-synuclein pathology can propagate from the gut to the brain, as hypothesized by Braak and his colleagues.

Here, we show that α-synuclein from a PD patient brain lysate is taken up and transported retrogradely over a long distance via the vagal nerves from the gut to the brain, after being injected into the wall of the gastrointestinal tract. We confirmed these observations using Atto-550-labeled recombinant α-synuclein forms (monomers, oligomers and fibrils). Additionally, we provide evidence that aggregated α-synuclein is transported by the fast component of microtubule-based axonal transport as well as in the slow component of axonal transport. Taken together, our findings strengthen the hypothesis that PD pathology may originate in the periphery and gradually propagate to the brain, where it eventually leads to PD.

Materials and Methods

Animals. Adult wild-type Sprague Dawley rats (approximately 250g) were purchased from Charles River Laboratories. Animals were kept with food and water *ad libitum* under a 12-h light/12-h dark cycle. Housing and procedures were conducted in accordance with ethical permit approved by Malmö-Lund Committee for animal research.

Preparation of brain lysates from PD patient. The patient died of acute aspiration and subsequent cardiac arrest due to advanced PD. Fresh substantia nigra was dissected out (20 hours post-mortem), immediately frozen and stored in -80 °C freezer until use. Lysates containing aggregated as well as mono- and oligomeric forms of α-synuclein were prepared with the freshly frozen substantia nigra tissue from the brain of a neuropathologically confirmed PD case (provided by Dr. Elisabet Englund, the Brain Bank, Lund University Hospital, Sweden). The tissue was homogenized at 10% (w/v) in sterile, phosphate-buffered saline (PBS) at 4 °C, vortexed, sonicated 3 x 5 seconds and centrifuged at 3000x g at 4 °C for 5 minutes. Supernatants were kept frozen at -80°C. The solution for injection was prepared by diluting the PD patient lysate supernatant before use to a final concentration of 3% (w/v). Different forms of α-synuclein (80μg/ml) were resuspended in PBS with or without fluorogold (40μg/ml).

Preparation of recombinant α-synuclein in monomeric, oligomeric, and fibrillar forms.

Expression and purification of recombinant α-synuclein. The expression and purification of human wild-type (WT) α-synuclein was performed as previously described [14]. Briefly, the Escherichia coli strain BL21 (DE3) (Stratagene, La Jolla, CA, USA) was transformed with

the expression vector pET3a encoding WT α-synuclein and the bacteria grown in LB medium to an optical density of 0.8. α-Synuclein expression was induced by 0.5mM IPTG for 3 h, the cells were lyzed by sonication and the cell lysates were clarified by centrifugation at 14000g, for 30 min. α-Synuclein was precipitated by 50% ammonium sulfate at 4 °C. The solution was spun at 4000 g, for 30 min at 4°C and the resulting pellet was resuspended in 10 mM Tris pH 7.5. The solution was loaded onto a DEAE column eluted by a gradient of 0–500 mM NaCl and the fractions containing α-synuclein (eluted at 200 mM NaCl), were heated to 75°C for 20 minutes. The solution was next clarified by centrifugation at 14000g, loaded onto a Superdex 75 HiLoad 26/60 column (GE healthcare), equilibrated and eluted in 50mM Tris–HCl, pH 7.5, 150mM KCl. Pure α-synuclein (0.2–0.5mM) in 50mM Tris–HCl, pH 7.5, 150mM KCl was filtered through sterile 0.22-μm filters and stored at -80°C. α-Synuclein concentration was determined spectrophotometrically using an extinction coefficient of $5960 M^{-1} cm^{-1}$ at 280 nm.

Assembly of monomeric α-synuclein into oligomers and fibrils. For oligomer formation, α-synuclein (200 μM) was incubated in buffer A (50mM Tris-HCl, pH 7.5, 150mM KCl) at 4°C, without shaking, for 7 days. Oligomeric α-synuclein was separated from the monomeric form of the protein by size exclusion chromatography (Superose 6 HR10/300, GE Healthcare). For fibril formation, α-synuclein was incubated in buffer A at 37°C under continuous shaking in an Eppendorf Thermomixer set at 600 r.p.m. Assembly was monitored continuously in a Cary Eclipse spectrofluorimeter (Varian Inc., Palo Alto, CA, USA) in the presence of Thioflavin T with excitation wavelength set at 440 and emissions wavelengths set at 480 and an averaging time of 1 s.

Fluorescent labeling of monomeric, oligomeric and fibrillar α-synuclein *assemblies and BSA.*

Monomeric and oligomeric α-synuclein assemblies in buffer A were buffer exchanged using NAP10 desalting columns (GE Healthcare) to phosphate buffered saline (PBS) buffer. We performed α-synuclein labeling with Atto-550 NHS ester fluorophore following the manufacturer's instructions (Atto-Tec Gmbh) using a protein:label molar ratio of 1:2 as such two Atto molecules per alpha-synucelin monomer whether monomeric, oligomeric or fibrillar form. The labeling reactions were arrested by addition of 1mM Tris pH 7.5. We removed unreacted fluorophore using NAP10 desalting columns. For fibrillar α-synuclein labeling, the fibrils were centrifuged twice at 15,000 *g* for 10 min, resuspended twice in PBS and labeled as described above. The unreacted fluorophore was removed by a final cycle of two centrifugations at 15,000 *g* for 10 min and resuspension of the pelleted fibrils in PBS. Lyophilized BSA was purchased form Sigma (A9418), dissolved in PBS at 5 mg/mL and labeled with ATTO-550 dye using a protein:dye ratio of 1:2 following the same procedure as described for monomeric α-synuclein.

Electron microscopy imaging. The nature of soluble, oligomeric and fibrillar α-synuclein forms was assessed using a JEOL 1400 transmission electron microscope following adsorption onto carbon-coated 200-mesh grids and negative staining with 1% uranyl acetate. The images were recorded with a Gatan Orius CCD camera (Gatan).

Operation procedures. Animals were anaesthetized using isofluorane (2-4%) and kept at a constant body temperature by the use of a heat pad. A schematic showing how the *in vivo* experiments were performed is depicted in Fig. 1. For each animal, injections were made using a 10µl Hamilton syringe into the intestine wall of stomach and duodenum at 5 sites, 1 cm apart. Injections were made in close proximity to the myenteric plexus. Each site was injected with 3µl of one of the four different forms of α-synuclein (PD brain lysate (2 µg/µl,

in total protein content), monomer (1 μg/μl), oligomer (1 μg/μl) or fibril (1 μg/μl), n=3 in each type and each time point). In addition control animals (n=3) were injected with BSA diluted (80 μg/ml) in phosphate buffered saline (PBS). Some of the animals were injected with a mixture of the synuclein forms and fluorogold. Following injection, animals were sutured and returned to normal housing conditions.

Tissue collection. After 12 (n=15), 24h (n=15), 72h (n=15) and 6 days (n=12) injected animals were anaesthetized with sodium pentobarbital and then transcardially perfused with 0.9% saline followed by fixation using ice-cold 4% paraformaldehyde (PFA) in PBS. A length of the vagal nerve, ranging from the brainstem to the diaphragm (~80 mm) as well as the brain and segments of the intestine were dissected and post-fixed in 4% PFA overnight. Tissues were then stored in 0.1 M PBS with 20% sucrose at 4°C. Transverse serial sections of the medulla oblongata, 30 μm thick, were cut in a microtome (Leica, SM 2010R). Vagal nerves were divided into proximal (0-15mm), medial (25-40mm) and distal (50-65mm) segments from the skull base, before entering the CNS. We then made transverse and longitudinal sections, 14μm, in a cryostat (Leica, CM 3050S) and mounted them on precoated glass slides. Slides were stored at -20°C before staining. Some sections were immediately separated, mounted on slides, coverslipped with PVA-DABCO and imaged for detection of the fluorescent tags of injected proteins.

Diaminobenzidine (DAB) staining. Freshly frozen tissue from PD patient was fixed with 4% PFA at room temperature for 10 minutes. The human brain sections and rat vagal nerve sections were stained on slides and after quenching in 3% H_20_2 in pure methanol, incubated with anti-α-synuclein LB 509 (mouse monoclonal, Life Technologies, 1:700), or anti--α-synuclein (mouse monoclonal, Santa Cruz Biotechnology, 1:1000) at 4°C, overnight. Then, the sections were incubated with a biotinylated anti-mouse secondary antibody (Vector, 1:400) at room temperature for 2 hours followed by incubation with ABC kit (Vectastain) and

DAB kit (Vector laboratories) conventional peroxidase system. Brightfield images were captured on a BX53 Olympus microscope.

Immunofluorescent labeling. We stained transverse sections of medulla oblongata as free-floating on a shaker while we stained vagal nerve sections on mounted glass slides using a primary antibody specific for human α-synuclein in order to detect transported α-synuclein. Sections were incubated with the following antibodies: anti-α-synuclein (mouse monoclonal, Santa Cruz 211, 1:1000), anti-choline acetyltransferase (goat, Millipore AB144P, 1:500) in combination with secondary antibodies; Alexa-555 anti-mouse (Jackson, 1:800), Alexa-488 anti-goat (Jackson, 1:800), FITC anti-rabbit (Jackson, 1:200). The confocal microscopic images of double-labeled medulla oblongata were captured using a Leica SP8 Scanning confocal microscope using a HyD detector using sequential scanning. Solid state lasers at wavelengths 488 nm and 552 nm were utilized to excite the respective fluorophores. The pinhole was retained at Airy 1 for all acquisitions. For each acquisition at the same magnification, identical settings were loaded for laser power gain. Post acquisition, deconvolution was performed using the "Deconvolution" plugin for ImageJ (developed by the Biomedical Imaging Group (BIG) - EPFL – Switzerland http://bigwww.epfl.ch/) utilizing the Richardson-Lucy algorithm and applying point-spreads functions (PSFs) calculated for the specific imaging equipment using the Gibson and Lanni model in the PSF Generator (BIG, EPFL – Switzerland http://bigwww.epfl.ch/algorithms/psfgenerator/). The same PSF models and deconvolution parameters were applied to all image stacks at the same magnification. Orthogonal projections were generated using ImageJ (v1.48p) without further modifications of the images.

Western Blotting

Tissue protein extraction. The substantia nigra of a Parkinson patient (advanced stage) was obtained from Lund Brain Bank, kindly supplied by Dr. Elisabet Englund. The sample was homogenized in the presence of proteases inhibitors using a FastPrep-24 homogenizer (MP Biomedicals, Santa Ana, CA, USA) in a lysis buffer 50 mM Tris/HCl pH7.4, 150 mM NaCl, 2 mM EDTA, 1% (v/v) NP-40, 0.1% (w/v) sodium dodecyl sulfate for further analysis by SDS-PAGE or in lysis buffer 20 mM Tris/HCl pH7.4, 100 mM NaCl, 0.4% (w/v) sodium dodecyl sulfate and 0.2% (v/v) Triton X-100 for Native-PAGE. Tissue homogenate was further sonicated twice for 10 s at 30% amplitude (QSonica, Newtown, CT, USA) with 1 min incubation on ice between each sonication step and centrifuged at 16000 g for 15 min at 4°C. The supernatant was recovered and protein concentration was quantified using BCA protein assay (Thermo Fisher Scientific, Rockford, IL, USA).

SDS-PAGE, Native PAGE and Western blotting analysis. Brain extract from a patient developing PD, monomeric, oligomeric and fibrillar α-syn were either mixed with SDS-PAGE loading buffer and heated to 100°C and analyzed on a 8-16% polyacrylamide gel or with Native-PAGE loading buffer and analyzed on a 8-16% polyacylamide. The samples were transferred to nitrocellulose membranes and probed with mouse anti-α-synuclein-1 antibody (S63320 BD Transduction Laboratories, 1:1000 dilution).

Cell culture, transfection and differentiation. Stable human neuroblastoma SH-SY5Y cells (passage 7-10) were maintained in DMEM Glutamax media (Gibco) supplemented with 10% FBS (Sigma) in a humidified 5% CO_2 atmosphere at 37°C. On the first day of the experiment 20 000 cells were seeded into the center wells of four well borosilicate glass chamber slides (Nunc) coated with matrigel (BD Bioscience), the remaining wells were filled with ddH_20 in order to avoid evaporation. The following day, cells were induced for neuronal differentiation by addition of 10μM retinoic acid (RA) to the medium. On day four of differentiation cells were transiently transfected using Lipofectamine 2000 (Life technologies) with plasmids

expressing bimolecular fluorescence complementation (BiFC) vectors of truncated (N- or C-terminus) or full length Venus fused to human wildtype α-synuclein [15] or Venus alone (kindly provided by Dr. Tiago Outerio, Göttingen, Germany). Actin-GFP was transfected in another group. The following day, media was replaced with fresh media supplemented with 10μM RA and 50 ng/ml BDNF, cells were then differentiated for four additional days

Live cell imaging, fluorescence recovery after photobleaching (FRAP) experiments and analyses. FRAP was performed using a Zeiss LSM 510 confocal microscope system running 2009 Zen software with 63x/1.4 Oil DIC Plan-apochromat objective and solid state 488 nm argon laser for excitation and bleaching of fluorophores. Constant temperature at 35-37°C, humidity and 5% CO_2 atmosphere was maintained using a heated stage and chamber system (CTI Controller 3700 digital, temp controller 37-2). FRAP was performed based on conventional FRAP procedure with minor modifications [3, 48]. Before each imaging session media were replaced with imaging buffer consisting of HBSS (Life technologies) supplemented with 5mM glucose, 1.8mM $CaCl_2$, 1mM $MgCl_2$ and 20mM HEPES, pH 7.4. Working at 256x256 pixel resolution, pre- and post-bleaching images were collected using 0.8% laser power to avoid photobleaching and phototoxicity at a rate of 5 Hz with pinhole set to maximum. Each experiment started with the collection of 4 baseline images. Bleaching was then performed with 100% laser power for 5 iterations within a circular field 100 μm in diameter, covering an area of the neurite located 100-200 μm away from the cell body. Following the photobleach, fluorescence intensities were recorded for 44 seconds in bleached, cell body reference and background regions. For each group; expressing α-synuclein-BiFC-Venus (n=4), α-synuclein-Venus (n=5), Actin-GFP (n=6) and Venus alone (n=5) three cells were imaged. Values averaged from the three cells in each experiment constitute one n. In order to investigate whether mobility was dependent on microtubule dynamics, separate experiments were then performed in which 10 nM of vinblastine was added to the media,

after one-hour incubation groups α-synuclein-BiFC-Venus (n=2), α-synuclein-Venus (n=3), Actin-GFP (n=5) and Venus alone (n=5) were imaged.

FRAP data analyses. Raw intensity signals were normalized, by subtracting the average background intensity for each time point (Supplementary Equation 1) as well as correcting for acquisition bleaching for each time point by adjusting to loss of fluorescence within the non-bleached reference region (Supplementary Equation 2, Supplementary Equation 3) [39]. The normalized data from each cell was then individually fitted to appropriate models. The type of model used for each protein were chosen in order to best describe the bleach corrected and normalized intensity data. For this, data from cells in α-synuclein-BiFC-Venus, α-synuclein-Venus and Actin-GFP groups were fitted to an exponential chemical-interaction model as described by equation (1) [39] as α-synuclein and actin are known to interact with other proteins. In contrast, vinblastine treated cells and those expressing Venus alone were fitted to the empirical diffusion model described by Ellenberg equation (3) [12]. From this, the mobile fraction was deduced with correction for gap ratio, equation (2). Fittings of FRAP curves that deviated significantly from normalized raw data were excluded from further analysis**.** All curve fittings and normalizations were performed in Igor Pro v6.32A using the plugin K_FRAPcalc v9 (developed by the European Advanced Light Microscopy Network (EAMNET) – EMBL – Germany http://www.embl.de/eamnet/).

$$I(t) = y_0 + Ae^{-\tau_1 t} \qquad (1)$$

(1) Single exponential model according to Phair single exponential, double normalization

$$Mob = \frac{\left(\frac{-A}{1-(y_0+A)}\right)}{Gap\ ratio} \qquad (2)$$

(2) For calculation of mobile fraction with correction for gap ratio

$$I(t) = I_{final}\left(1 - \left(\frac{w^2}{w^2 + 4\pi Dt}\right)^{½}\right) \qquad (3)$$

(3) Ellenberg – I final will be considered the mobile fraction.

Statistical Analysis

All data were analyzed using GraphPad Prism software (developed by GraphPad Software, San Diego, USA http://www.graphpad.com). FRAP groups were analyzed by one-way ANOVA for difference among the groups, then groups in-between were compared pairwise by student's *t*-test.

Figures and artwork

Vector graphics and schematics were created using Adobe illustrator CS5 and figures arranged and compiled using Adobe InDesign CS5.

Results

α-Synuclein from a PD patient lysate is transported via the vagal nerve from the intestine to the brain.

α-Synuclein is an abundant protein in the neuron. In the brain of PD patients, the protein is misfolded and aggregated, forming Lewy bodies and Lewy neurites in dopaminergic neurons of the substantia nigra as well as in other types of neuron in different brain regions. We first

collected fresh substantia nigra tissue from a neuropathologically confirmed Parkinsonian case. Immunohistochemical analysis confirmed the presence of distinct α-synuclein-positive Lewy body structures in brain sections (Fig. 1a). This tissue was therefore used for PD brain lysate preparation. Furthermore, we performed biochemical analyses of the brain lysate preparation in order to assess the different forms of α-synuclein it contained. In denaturing conditions, in the presence of SDS, α-synuclein appears monomeric with a molecular weight of ~17kDa (Fig. 1b); whilst the native PAGE reveals the presence of higher molecular α-synuclein forms in the brain lysate (Fig. 1b).

After confirming the presence of the α-synuclein forms in the lysate, we injected 3 µl of this lysate (2 µg/µl, total protein) into the intestine of wildtype adult rats (Fig. 1c) and assessed the presence of α-synuclein in the vagal nerve by immunohistochemistry using an antibody that specifically recognizes human α-synuclein (*See: Experimental procedures*). We detected distinct α-synuclein immunoreactivity in the intestinal wall (Fig. 1d, middle panel) and in the vagal nerve at time-dependent matter (12, 48, and 72 hours post-injections) (Fig. 2, middle panel). No human α-synuclein was detected in the controls, which were injected with bovine serum albumin (BSA) (Fig. 1d, Fig. 2). When a BSA antibody was used, no distinct immunoreactivity was detected in the vagal nerves at different time points (Supplement Fig. 1).

Together, these experiments demonstrate that the PD brain lysate contains different α-synuclein forms, and they show that α-synuclein from the injected lysate is taken up and transported via the vagal nerve to the brain. In contrast, although BSA is present in the injection site of the intestinal wall, it is not taken up and transported into the vagal nerve.

Different α-synuclein forms are transported from the intestine to the brain via the vagal nerve

We have shown that the brain lysate contains a mixture of monomeric, oligomeric and fibrillar α-synuclein forms. However, it is not clear which form(s) of the protein is taken up and transported to the vagal nerve. Thus, we performed the experiments with distinct, characterized α-synuclein forms. These were fluorescently labeled in order to allow direct visualization; we determined the nature of each α-synuclein form by SDS-PAGE and native PAGE (Fig. 1b) and transmission electron microscopy (Fig. 4a). Size exclusion chromatography analyses further revealed the defined and size-specific forms of α-synuclein used in the experiments (Fig. 4b).

When aggregated α-synuclein in the form of fibrils were injected, we observed distinct α-synuclein in the intestinal wall (Fig. 1d) and in the vagal nerve at time-dependent manner (Fig. 2), similar to the PD brain lysate. Particularly, in the high power images, we could clearly see intensely immune-stained nerve fibers of the vagal nerves in the PD brain lysate- and fibril-injected animals (Fig. 3). In order to verify that different forms of α-synuclein are indeed transported from the intestines to the brain, we injected monomeric-, oligomeric- or fibrillar Atto-550-α-synuclein with fluorogold, (a live dye, used as a control for the injection) into the intestinal wall of the adult rats. Forty-eight hours later, we detected fluorogold and Atto-550 positive fluorescent punctae in neurons in the DMV, for monomeric-, oligomeric and fibrillar forms of α-synuclein we injected. Most, if not all, Atto-550-α-synuclein positive structures overlapped with fluorogold fluorescence (Supplement Fig. 2a-c). When fluorogold was co-injected with unlabeled PD brain lysate, no Atto-550 fluorescence was observed (Supplement Fig. 2d). These data strongly indicate that the human α-synuclein found in the neurons of the DMV was transported from the injected sites within the intestine.

The neurons of the DMV are cholinergic. To further verify that the human α-synuclein in the DMV is transported from the gastrointestinal wall via the vagal nerve, we double-stained

brain sections of medulla oblongata with antibodies against the phenotypic cholinergic enzyme, choline acetyltransferase (ChAT) and human α-synuclein. In samples collected 6 days after intestinal injection, nearly all neurons positively stained for human α-synuclein were also positive for ChAT (Fig. 5b-e). In contrast, no α-synuclein immunoreactivity was detected in controls (BSA-injected animals; Fig. 5a). Interestingly, the animals sacrificed 24 hours post-injection did not show any human α-synuclein immunoreactivity in ChAT-positive neurons in the DMV region (Supplement Fig. 3). These data further suggest that different α-synuclein forms are transported over a long distance from the intestine to the brain in a time-dependent manner.

Transport pattern of aggregating α-synuclein.

α-Synuclein is a soluble, unfolded protein, which forms α-helical structures when membrane-bound. Previously, we demonstrated that the majority of soluble α-synuclein is located within the cytosol and transports via slow axonal transport, including slow component a (SCa) and slow component b (SCb), while a small fraction (about one quarter) of the total cellular α-synuclein is membrane-associated and transports through fast axonal transport, i.e. the fast component [19]. Membrane-bound α-synuclein is α-helical and does not contribute to aggregation and fibrillation, while the soluble form of the protein populates folding intermediates that oligomerize and assemble into fibrils. Our *in vivo* experiments show that monomeric, oligomeric and fibrillar forms of α-synuclein are retrogradely transported from the intestine to the brain via the vagal nerve. However, it is not clear which machinery is involved in the transport of different α-synuclein forms, especially the aggregated ones (oligomers and fibrils), which likely contribute to pathology of PD [10, 34, 50]. As live-cell imaging would be technically challenging to perform in living animals, we used an *in vitro*

system where cultured differentiated neuroblastoma cells (from the SH-SY5Y line), which exhibit neuronal morphology, were transfected with α-synuclein constructs expressing human α-synuclein tagged with full length fluorescent protein (Venus) or co-transfected with Bimolecular Fluorescence Complementation (BiFC) truncated parts of a Venus, which upon dimerization and oligomerization of α-synuclein reveals fluorescence [15, 35]. Taking advantage of this system that allows us to visualize both total α-synuclein and specifically the aggregated α-synuclein with complemented fluorescence, we performed fluorescence recovery after photobeaching (FRAP) experiments in differentiated SH-SY5Y cells (Fig. 6a-b, Supplement Fig. 5a). Functionality of axons in differentiated cells was validated by transfection using a mito-GFP construct (Supplement Fig. 4b).

In order to study the motility of aggregating α-synuclein, we first asked whether the transport of aggregated α-synuclein in neurons occurs by an active process (protein-protein interaction) or by passive diffusion. We use two distinct models that represent these forms of transport, respectively. Cells, expressing full-length Venus alone (empty vector) or actin-GFP were used as controls. Venus alone, being a freely diffusing protein independent of molecular interactions, displayed a complete recovery of signal following photobleaching returning to the pre-bleach level ($p<0.0001$) as expected. In contrast we observed α-synuclein-Venus and the complemented α-synuclein-BiFC-Venus signal to recover only to 75% of the pre-bleach intensity ($p<0.0017$). Actin-GFP showed a much lower recovery ($p<0.0002$), typical of a low motility protein dependent on protein-protein interaction. This was also expected, as actin has been documented to be primarily transported in SCb [4] The rapid, but partial, recovery of complemented α-synuclein-BiFC-Venus suggests that it is involved in protein-protein interaction (Fig. 6b, c). As expected similar results were seen for total α-synuclein-Venus.

Fast axonal transport is microtubule-based, and microtubule itself is transported in SCa. In order to investigate whether transport of aggregated α-synuclein was microtubule dependent we treated the cultures with 10nM vinblastine, an agent known to destabilize microtubules[2, 20], for one hour before the FRAP experiment. The treatment affected neither the protein-mobility of actin-GFP nor that of Venus alone (p = 0.1586 and p = 0.1618, respectively). No increase in mobility was observed for α-synuclein-Venus reflecting the whole pool of protein regardless of being interacted to subcellular components or not (e.g. membrane bound, microtubule or soluble). The BiFC approach offers the unique opportunity to exclusively visualize the aggregating (oligomeric) form of α-synuclein. In this group we observed a significant increase in mobility (Fig. 6d, p =0.00948). The level of mobility of aggregated α-synuclein in vinblastine treated cells was comparable to that of free diffusion, as seen in cells expressing Venus alone (Fig. 6d, p = 0.64074).. This 25% increase, for oligomeric α-synuclein, following vinblastine treatment shows that aggregated α-synuclein is directly interacting with microtubule in functional axons of neuron-like cells, suggesting aggregated α-synuclein is likely transported both by the fast component (microtubule-based) as well as SCa and SCb.

Discussion

In the present study we demonstrate that aggregated α-synuclein is transported from the intestine to the brain. Our *in vitro* data also suggests that aggregated α-synuclein is transported through both fast and slow axonal transports.

α-synuclein and its aggregated forms are transported in long-distance from the intestine to the brain

After intensive studies, Braak and colleagues proposed the six stages of neuropathology during PD pathogenesis [6-8]. The first sign of Lewy pathology appears in the projection neurons of the dorsal motor nucleus of the vagus at the early stage of PD [9]. Later on, the vulnerable brain regions are affected in a predictable sequence, progressing in a stereotypical caudal-rostral pattern starting in the lower brainstem, medulla oblongata, and exhibiting the pathology in more rostral regions later. A key question is how this step-wise temporal appearance is developed over time (over many years in humans). Braak hypothesized that the Lewy pathology retrogradely progresses from the intestine to the brain. However, some studies have argued against the findings of the Braak hypothesis, by showing non-stereotypic patterns of Lewy pathology [18, 37, 38]. In the present study, we provide direct evidence that retrogradely transported α-synuclein forms indeed lead to spread of the Lewy pathology from the peripheral tissue (gastro-intestinal) to the brain via the vagal nerve. Similar phenomena are observed not only for monomeric α-synuclein, but also for oligomeric and fibrillar α-synuclein, the latter most likely being a significant contributor to the Lewy pathology propagation in PD conditions. The vagal route of α-synuclein transport has also been documented by systemic administration of the environmental toxin rotenone [36], as well as by directly injecting adeno-associated viral vectors overexpressing human α-synuclein into the vagal nerve [49]. The clear difference between the present study and previous work is that exogenous α-synuclein forms are not readily detected in the vagal nerves/neurons and the brain parenchyma [15, 31, 32, 49].

After being delivered to the gastrointestinal wall, α-synuclein must first be taken up into the vagal nerve terminals or indirectly to the enteric neurons and/or their terminals first, then trans-synaptically transfer via the synapses between the enteric neurons and the vagal nerves to reach the brain. Thus, the amount of transported α-synuclein is expected to be low. We found that all α-synuclein forms (monomers, oligomers and fibrils) are actively transported

from the intestine to the dorsal motor nucleus of the vagus. It is therefore conceivable that the gut-to-brain route is an important route for α-synuclein propagation. The protein is taken up into the peripheral tissues and is transported to the lower brain. The spread of pathology is time-dependent. Figure 6 illustrates the overview pattern of α-synuclein transport between the intestine and the brain. We readily observed distinct α-synuclein in the intestinal wall shortly (12 hours) after injection, however, at the same time, we barely detected any α-synuclein in the vagal nerve, which became evident in the later time points. Correspondently, we did not detect any human α-synuclein in the DMV 24 hours after the injection while considerable numbers of α-synuclein-positive neurons were observed in the later time points (72-144 hours) after the injection. Although we did notice a stronger α-synuclein-positive signal in the DMV of animals injected with monomeric and oligomeric α-synuclein compared to those injected with fibrillar form or PD brain lysate, suggesting a difference in propensity to transport, we hesitate for such conclusions since transport most likely also depend on the success and favorable quality of injection sites in each animal. Several groups elegantly showed that α-synuclein pathology spread along the neuronal connections after injecting the PD brain lysate, transgenic mouse brain lysate or preformed α-synuclein fibrils in the striatum and the cortex of mice or monkeys [31, 32, 42, 43], where the exogenous α-synuclein induced a seeding effect of endogenous α-synuclein, suggesting a permissive templating prion-like process [16]. The time-dependent and connectivity-dependent spread of the Lewy pathology is closely accompanied by dopaminergic neuronal cell death at 90 and 180 days post-injection [31]. It is worth mentioning that we also examined potential cell death in the DMV with cell death markers, such as activated caspase 3, and α-synuclein presence in higher brain regions, such as the locus coeruleus and the substantia nigra. We did not detect distinct dying cells, nor exogenous α-synuclein in these brain regions (data not shown). The discrepancy between

our findings and theirs could be due to the dose of delivered α-synuclein and incubation time (6 days vs. 90-180 days) following injection.

The mechanisms of transport of α-synuclein species

Sufficient axonal transport is essential for neuronal function. Based on the speed of the trafficking, axonal transport is categorized into fast axonal transport (largely involved in membrane-bound organelles) with rates of 50-400 mm/day and slow axonal transports (SCa and SCb). SCa transports microtubules and neurofilaments at average rate of about 1 mm/day, while SCb transports handful soluble cytosolic proteins, including actin at average rate of about 2-8 mm/day [47]. Roy and his co-workers reported that α-synuclein was transported in SCb. It appeared that α-synuclein co-transported with other SCb proteins [44-46] Using stop-flow/nerve crush operations and metabolic labeling of retinal ganglion cells, we demonstrated that (monomeric) α-synuclein is transported by all axonal transport components (fast transport, SCa and SCb) and that the majority of protein is transported through SCa and SCb, while one quarter is transported through fast axonal transport [19]. The oligomeric form of α-synuclein impairs microtubule-kinesin interaction and lead to early neurite pathology[41] and oligomeric and/or fibrillar α-synuclein is the vector of pathology propagation [1, 31, 42]. It is thus essential to understand the transport mechanism of oligomeric and fibrillar α-synuclein in neurons. *In vitro* studies with microfluidic chambers showed that preformed α-synuclein fibrils were not only taken up and transported within primary neurons but also transmitted to secondary neurons [13, 33]. Taking advantage of the unique strategy of BiFC, with the FRAP technique, we demonstrated that oligomeric α-synuclein and likely the fibrillar form as well, is directly associated with microtubule plausibly engaged in active transport. Likely, the aggregated forms of α-synuclein are involved in all form of axonal transports, as for

onomeric α-synuclein by associating with fast transporting cargoes, interacting with microtubules and staying in soluble states. At certain conditions, such as phosphorylation or truncations, they may translocate from one subcellular compartment to another. Furthermore, we also demonstrated that assembled α-synuclein is retrogradely transported along long-distance ranges from the intestine to the brain. Given the fact that the full vagal nerve length is about 110-140 mm in adult rats from the DMV to the muscles in the intestine wall our *in vivo* findings suggest an average translocation rate of 20-30 mm/day i.e. faster than SCb in the reported range of fast microtubule associated transport [24], in support of multi-phasic transport. The actual transport rate is most likely faster as the estimated rate also covers the time required for accumulation of α-synuclein in the cell body in the DMV as well as time required for α-synuclein direct or indirect uptake into the axon of the projecting nerve cell. Because of the limitations of FRAP, specific membranous cargoes or transport motors that are involved in the transport of α-synuclein are yet to be evaluated.

The long-range anterograde and retrograde transport of α-synuclein assemblies may contribute to a complex spread of Lewy pathology. Numerous experimental evidences, including our present findings, support Braak's hypothesis that α-synuclein is transported retrogradely. Nonetheless, discrepant findings [18, 38] indicate diverse clinical features for PD with different subtypes of neuropathology. In an independent study we recently demonstrated that aggregated α-synuclein is also transported anterogradely in neurons, for example, from the cortex to the spinal cord (Unpublished observations). The bidirectional transport of α-synuclein assemblies may account for the complexity of PD pathology.

Acknowledgements

The authors wish to thank Marianne Juhlin and AnnaKarin Oldén for their excellent technical support. We thank Andrew C. McCourt for the linguistic revision of this manuscript. This work was funded by grants from the Swedish Research Council; Torsten Söderberg Foundation and Swedish Parkinson Foundation (J.-Y. L.). S.H., O.C., T.A., L.R. and J.-Y. L are active and supported by BAGADILICO - Excellence in Parkinson and Huntington Research, and the Strategic Research Area Multipark (Multidisciplinary research in Parkinson's disease at Lund University); L.B. and R.M. are supported by the Centre National de la Recherche Scientifique and grants from the Agence Nationale de la Recherche (ANR-11-BSV8-021-01) and a 'Coup d'Elan a la Recherche Francaise' award from Fondation Bettencourt Schueller. Z.Y.W. and J.-Y.L. are supported by National Natural Science Foundation of China (81430025) and the Fundamental Research Funds for Central Universities of China (N130120002).

The authors declare no competing financial interests.

References

1 Aguzzi A, Rajendran L (2009) The transcellular spread of cytosolic amyloids, prions, and prionoids. Neuron 64: 783-790

2 Ahmad FJ, Echeverri CJ, Vallee RB, Baas PW (1998) Cytoplasmic dynein and dynactin are required for the transport of microtubules into the axon. J Cell Biol 140: 391-401

3 Axelrod D, Koppel DE, Schlessinger J, Elson E, Webb WW (1976) Mobility measurement by analysis of fluorescence photobleaching recovery kinetics. Biophys J 16: 1055-1069 Doi S0006-3495(76)85755-4 [pii] 10.1016/S0006-3495(76)85755-4

4 Black MM, Lasek RJ (1979) Axonal transport of actin: slow component b is the principal source of actin for the axon. Brain Res 171: 401-413

5 Braak H, de Vos RA, Bohl J, Del Tredici K (2006) Gastric alpha-synuclein immunoreactive inclusions in Meissner's and Auerbach's plexuses in cases staged for Parkinson's disease-related brain pathology. Neurosci Lett 396: 67-72

6 Braak H, Del Tredici K (2009) Neuroanatomy and pathology of sporadic Parkinson's disease. Adv Anat Embryol Cell Biol 201: 1-119

7 Braak H, Del Tredici K, Rub U, de Vos RA, Jansen Steur EN, Braak E (2003) Staging of brain pathology related to sporadic Parkinson's disease. Neurobiol Aging 24: 197-211

8 Braak H, Ghebremedhin E, Rub U, Bratzke H, Del Tredici K (2004) Stages in the development of Parkinson's disease-related pathology. Cell Tissue Res 318: 121-134
9 Braak H, Rub U, Gai WP, Del Tredici K (2003) Idiopathic Parkinson's disease: possible routes by which vulnerable neuronal types may be subject to neuroinvasion by an unknown pathogen. J Neural Transm 110: 517-536
10 Danzer KM, Haasen D, Karow AR, Moussaud S, Habeck M, Giese A, Kretzschmar H, Hengerer B, Kostka M (2007) Different species of alpha-synuclein oligomers induce calcium influx and seeding. J Neurosci 27: 9220-9232
11 Desplats P, Lee HJ, Bae EJ, Patrick C, Rockenstein E, Crews L, Spencer B, Masliah E, Lee SJ (2009) Inclusion formation and neuronal cell death through neuron-to-neuron transmission of alpha-synuclein. Proc Natl Acad Sci U S A 106: 13010-13015
12 Ellenberg J, Siggia ED, Moreira JE, Smith CL, Presley JF, Worman HJ, Lippincott-Schwartz J (1997) Nuclear membrane dynamics and reassembly in living cells: targeting of an inner nuclear membrane protein in interphase and mitosis. J Cell Biol 138: 1193-1206
13 Freundt EC, Maynard N, Clancy EK, Roy S, Bousset L, Sourigues Y, Covert M, Melki R, Kirkegaard K, Brahic M (2012) Neuron-to-neuron transmission of alpha-synuclein fibrils through axonal transport. Ann Neurol 72: 517-524 Doi 10.1002/ana.23747
14 Ghee M, Melki R, Michot N, Mallet J (2005) PA700, the regulatory complex of the 26S proteasome, interferes with alpha-synuclein assembly. FEBS J 272: 4023-4033
15 Hansen C, Angot E, Bergstrom AL, Steiner JA, Pieri L, Paul G, Outeiro TF, Melki R, Kallunki P, Fog Ket al (2011) alpha-Synuclein propagates from mouse brain to grafted dopaminergic neurons and seeds aggregation in cultured human cells. J Clin Invest 121: 715-725 Doi 10.1172/JCI43366 43366 [pii]
16 Hardy J (2005) Expression of normal sequence pathogenic proteins for neurodegenerative disease contributes to disease risk: 'permissive templating' as a general mechanism underlying neurodegeneration. Biochem Soc Trans 33: 578-581
17 Hawkes CH, Del Tredici K, Braak H (2009) Parkinson's disease: the dual hit theory revisited. Ann N Y Acad Sci 1170: 615-622
18 Jellinger KA (2008) A critical reappraisal of current staging of Lewy-related pathology in human brain. Acta Neuropathol 116: 1-16
19 Jensen PH, Li JY, Dahlstrom A, Dotti CG (1999) Axonal transport of synucleins is mediated by all rate components. Eur J Neurosci 11: 3369-3376
20 Jordan MA, Wilson L (2004) Microtubules as a target for anticancer drugs. Nat Rev Cancer 4: 253-265 Doi 10.1038/nrc1317 nrc1317 [pii]
21 Kordower JH, Chu Y, Hauser RA, Freeman TB, Olanow CW (2008) Lewy body-like pathology in long-term embryonic nigral transplants in Parkinson's disease. Nat Med 14: 504-506
22 Kordower JH, Chu Y, Hauser RA, Olanow CW, Freeman TB (2008) Transplanted dopaminergic neurons develop PD pathologic changes: a second case report. Mov Disord 23: 2303-2306
23 Kurowska Z, Englund E, Widner H, Lindvall O, Li J-Y, Brundin P (2011) Signs of Degeneration in 12-22-Year Old Grafts of Mesencephalic Dopamine Neurons in Patients with Parkinson's Disease. Journal of Parkinsons Disease 1: 83-92 Doi 10.3233/jpd-2011-11004
24 Lasek RJ, Garner JA, Brady ST (1984) Axonal transport of the cytoplasmic matrix. Journal of Cell Biology 99: 212-221
25 Lebouvier T, Chaumette T, Paillusson S, Duyckaerts C, Bruley des Varannes S, Neunlist M, Derkinderen P (2009) The second brain and Parkinson's disease. Eur J Neurosci 30: 735-741
26 Lee HJ, Suk JE, Lee KW, Park SH, Blumbergs PC, Gai WP, Lee SJ (2011) Transmission of Synucleinopathies in the Enteric Nervous System of A53T Alpha-Synuclein Transgenic Mice. Exp Neurobiol 20: 181-188 Doi 10.5607/en.2011.20.4.181
27 Lee HJ, Suk JE, Patrick C, Bae EJ, Cho JH, Rho S, Hwang D, Masliah E, Lee SJ (2010) Direct transfer of alpha-synuclein from neuron to astroglia causes inflammatory responses in synucleinopathies. J Biol Chem 285: 9262-9272
28 Lerner A, Bagic A (2008) Olfactory pathogenesis of idiopathic Parkinson disease revisited. Mov Disord 23: 1076-1084

29 Li JY, Englund E, Holton JL, Soulet D, Hagell P, Lees AJ, Lashley T, Quinn NP, Rehncrona S, Bjorklund Aet al (2008) Lewy bodies in grafted neurons in subjects with Parkinson's disease suggest host-to-graft disease propagation. Nat Med 14: 501-503 Doi nm1746 [pii] 10.1038/nm1746
30 Li JY, Englund E, Widner H, Rehncrona S, Bjorklund A, Lindvall O, Brundin P (2010) Characterization of Lewy body pathology in 12- and 16-year-old intrastriatal mesencephalic grafts surviving in a patient with Parkinson's disease. Mov Disord 25: 1091-1096 Doi 10.1002/mds.23012
31 Luk KC, Kehm V, Carroll J, Zhang B, O'Brien P, Trojanowski JQ, Lee VM (2012) Pathological alpha-synuclein transmission initiates Parkinson-like neurodegeneration in nontransgenic mice. Science 338: 949-953 Doi 10.1126/science.1227157 338/6109/949 [pii]
32 Luk KC, Kehm VM, Zhang B, O'Brien P, Trojanowski JQ, Lee VM (2012) Intracerebral inoculation of pathological alpha-synuclein initiates a rapidly progressive neurodegenerative alpha-synucleinopathy in mice. J Exp Med 209: 975-986 Doi jem.20112457 [pii] 10.1084/jem.20112457
33 Luk KC, Song C, O'Brien P, Stieber A, Branch JR, Brunden KR, Trojanowski JQ, Lee VM (2009) Exogenous {alpha}-synuclein fibrils seed the formation of Lewy body-like intracellular inclusions in cultured cells. Proc Natl Acad Sci U S A 106: 20051-20056
34 Nonaka T, Watanabe ST, Iwatsubo T, Hasegawa M (2010) Seeded aggregation and toxicity of {alpha}-synuclein and tau: cellular models of neurodegenerative diseases. The Journal of biological chemistry 285: 34885-34898 Doi 10.1074/jbc.M110.148460
35 Outeiro TF, Putcha P, Tetzlaff JE, Spoelgen R, Koker M, Carvalho F, Hyman BT, McLean PJ (2008) Formation of toxic oligomeric alpha-synuclein species in living cells. PLoS ONE 3: e1867
36 Pan-Montojo F, Schwarz M, Winkler C, Arnhold M, O'Sullivan GA, Pal A, Said J, Marsico G, Verbavatz JM, Rodrigo-Angulo Met al (2012) Environmental toxins trigger PD-like progression via increased alpha-synuclein release from enteric neurons in mice. Sci Rep 2: 898 Doi 10.1038/srep00898
37 Parkkinen L, Kauppinen T, Pirttila T, Autere JM, Alafuzoff I (2005) Alpha-synuclein pathology does not predict extrapyramidal symptoms or dementia. Ann Neurol 57: 82-91
38 Parkkinen L, Pirttila T, Alafuzoff I (2008) Applicability of current staging/categorization of alpha-synuclein pathology and their clinical relevance. Acta Neuropathol:
39 Phair RD, Gorski SA, Misteli T (2004) Measurement of dynamic protein binding to chromatin in vivo, using photobleaching microscopy. Methods Enzymol 375: 393-414
40 Phillips RJ, Walter GC, Wilder SL, Baronowsky EA, Powley TL (2008) Alpha-synuclein-immunopositive myenteric neurons and vagal preganglionic terminals: autonomic pathway implicated in Parkinson's disease? Neuroscience 153: 733-750
41 Prots I, Veber V, Brey S, Campioni S, Buder K, Riek R, Bohm KJ, Winner B (2013) alpha-Synuclein oligomers impair neuronal microtubule-kinesin interplay. J Biol Chem 288: 21742-21754 Doi 10.1074/jbc.M113.451815 M113.451815 [pii]
42 Recasens A, Dehay B, Bove J, Carballo-Carbajal I, Dovero S, Perez-Villalba A, Fernagut PO, Blesa J, Parent A, Perier Cet al (2014) Lewy body extracts from Parkinson disease brains trigger alpha-synuclein pathology and neurodegeneration in mice and monkeys. Ann Neurol 75: 351-362 Doi 10.1002/ana.24066
43 Rey NL, Petit GH, Bousset L, Melki R, Brundin P (2013) Transfer of human alpha-synuclein from the olfactory bulb to interconnected brain regions in mice. Acta Neuropathol 126: 555-573 Doi 10.1007/s00401-013-1160-3
44 Roy S, Winton MJ, Black MM, Trojanowski JQ, Lee VM (2008) Cytoskeletal requirements in axonal transport of slow component-b. J Neurosci 28: 5248-5256
45 Roy S, Winton MJ, Black MM, Trojanowski JQ, Lee VM (2007) Rapid and intermittent cotransport of slow component-b proteins. J Neurosci 27: 3131-3138
46 Scott DA, Das U, Tang Y, Roy S (2011) Mechanistic logic underlying the axonal transport of cytosolic proteins. Neuron 70: 441-454 Doi S0896-6273(11)00295-9 [pii] 10.1016/j.neuron.2011.03.022

47 Shea TB, Flanagan LA (2001) Kinesin, dynein and neurofilament transport. Trends Neurosci 24: 644-648

48 Snapp EL, Altan N, Lippincott-Schwartz J (2003) Measuring protein mobility by photobleaching GFP chimeras in living cells. Curr Protoc Cell Biol Chapter 21: Unit 21 21 Doi 10.1002/0471143030.cb2101s19

49 Ulusoy A, Rusconi R, Perez-Revuelta BI, Musgrove RE, Helwig M, Winzen-Reichert B, Di Monte DA (2013) Caudo-rostral brain spreading of alpha-synuclein through vagal connections. EMBO Mol Med 5: 1051-1059 Doi 10.1002/emmm.201302475

50 Winner B, Jappelli R, Maji SK, Desplats PA, Boyer L, Aigner S, Hetzer C, Loher T, Vilar M, Campioni Set al (2011) In vivo demonstration that alpha-synuclein oligomers are toxic. Proceedings of the National Academy of Sciences of the United States of America 108: 4194-4199 Doi 10.1073/pnas.1100976108

Figure Legends

Fig. 1 Characterization of α-Synuclein forms from PD brain lysate and recombinant proteins injected into the intestinal wall. a. A section of the substantia nigra of the PD patient that the brain lysate for injection was generated from were subjected to immunohistochemistry with an antibody specifically against human α-synuclein. The low power image shows an overview of Lewy pathology (scale bar = 30 μm). The high power image (inset) shows detail of distinct Lewy body (scale bar = 10 μm). b. Western blotting showing components of α-synuclein forms in PD patient brain lysate and monomeric, oligomeric or fibrillar α-synuclein form in SDS-PAGE (8-16% polyacrylamide gel) or Native PAGE (8-16% polyacrylamide gel). α-synuclein shows as one band at ~ 17kDa in SDS-PAGE. Smear in the Native-PAGE indicates the presence of different α-synuclein forms in the brain lysate (1) and synthetic α-synuclein fibrils (4). The band labeled with a star corresponds to a protein recognized by the secondary anti-mouse HRP antibody. c. Overview of the injection sites and pathways interconnecting between the central nervous system and the enteric nervous system. DMV: dorsal motor nucleus of the vagus.. SNpc: substantia nigra pars compacta. SNpr: substantia nigra pars reticulata. HN: hypoglossal nucleus. d. Immunohistochemical images of the intestines 12 hours after injecting BSA (left), PD brain lysate (middle) and fibrils (right) when the sections are immune-stained with an α-synuclein antibody (syn211, upper panels) or with an antibody against BSA (low panels). Distinct α-synuclein immunoreactivities were observed in the PD lysate or α-synuclein fibril injected intestines, while distinct BSA immunoreactivity was detected in the BSA injected intestines. Scale bars, 100 μm for low power images, 50 μm for high power images**.**

Fig. 2. Time-dependent transport of α-synuclein in the vagal nerve. Schematic drawing on the left illustrating the vagal nerve segments dissected between the skull base and the level of the diaphragm. The actual levels of the segments are shown on the right. Rats received injections of BSA (left), PD lysate (middle) or α-synuclein fibrils (right). The sections of vagal nerves were immunostained with an antibody against human α-synuclein. a. 12 hours after the injection, no distinct α-synuclein immunoreactivity was observed in segments of the vagal nerves from PD lysate or α-synuclein fibrils injected rats. b. 48 hours after injections distinct α-synuclein immunoreactivity was observed in nerve fibers of the vagal nerves from PD lysate or α-synuclein fibrils injected rats, in contrast to the vagal nerve injected with BSA in the intestines. c. 72 hours after injections, (similar to b), distinct α-synuclein immunoreactivity was observed in nerve fibers of the vagal nerves from PD lysate or α-synuclein fibrils injected rats. Scale bars = 50 μm.

Fig. 3. High power images of α-synuclein immunoreactivity in sections of vagus nerve 12 hours (a), 48 hours (b) and 72 hours (c) after the injection. Rats received injections of BSA (left), PD lysate (middle) or α-synuclein fibrils (right). a. No distinct α-synuclein immunoreactivity was observed in segments of the vagal nerves from PD lysate or α-synuclein fibrils injected rats, 12 hours after the injection. b. Distinct α-synuclein immunoreactivity was observed in nerve fibers of the vagal nerves from PD lysate or α-synuclein fibrils injected rats, in contrast to the vagal nerve injected with BSA in the intestines, 48 hours after injections. c. Similar to b, distinct α-synuclein immunoreactivity was observed in nerve fibers of the vagal nerves from PD lysate or α-synuclein fibrils injected rats, 72 hours after injections. Scale bar = 20 μm.

Fig. 4. Characterization of α-synuclein forms. a. Negatively stained transmission electron micrographs of monomeric, oligomeric and fibrillar α-synuclein. (Scale bar represents 200 nm). b. Size exclusion chromatography analysis of monomeric and oligomeric α-synuclein. Elution profile of pure recombinant monomeric (Top) oligomerized α-synuclein (Middle) and oligomeric α-synuclein incubated 7 days at 4°C, from a Superose 6 (HR 10/30) column (Bottom). Arrows show the location of oligomeric and monomeric α-synuclein. Solid arrowheads show the location of molecular size markers (thyroglobulin, 670 kDa; immunoglobulin G, 158 kDa; ovalbumin, 44 kDa and myoglobin, 17 kDa) run under identical conditions on the same column.

Fig. 5. Atto-550-α-Synuclein forms specifically transported into the DMV, 144 hours after injection into the wall of the intestine. In order to enhance the signal the brain sections were immunostained with antibodies directed specifically against human α-synuclein (Syn211, red, a-e, a''-d'', a'''-e''')) and ChAT (green, a-e, a'-d', a'''-e'''), the phenotypic markers of the DMV. Monomeric (b), oligomeric (c), fibrillar (d) α-synuclein and PD patient brain lysate (e) injected animals display double labeled neurons (arrows), while BSA injection does not yield any α-synuclein positive neurons (a''). Scale Bars, 25 μm in a-e, and 10 μm in a'''-e'''.

Fig. 6. Mechanisms of transport of α-synuclein assemblies. a. A schematic drawing showing how the FRAP experiment was performed. To the right representative images of neurite before, during and after fluorescent recovery b. Raw, unfitted, FRAP curves for three representative cells expressing complemented α-synuclein-BiFC-Venus, actin-GFP or Venus alone. c. Normalized and summarized data from fitted curves for mobility of complemented

α-synuclein-BiFC-Venus, α-synuclein-Venus, actin-GFP or Venus alone. d. data for mobility of same with treatment with 10nM vinblastine. * $p<0.05$; $p<0.0002$; $p<0.0001$.

Fig. 7. An overview of uptake and transport of BSA and α-synuclein in the PD brain lysate or synthetic recombinant α-synuclein fibrils, in the intestines, along the vagal nerve and in the medulla oblongata, at different time points.

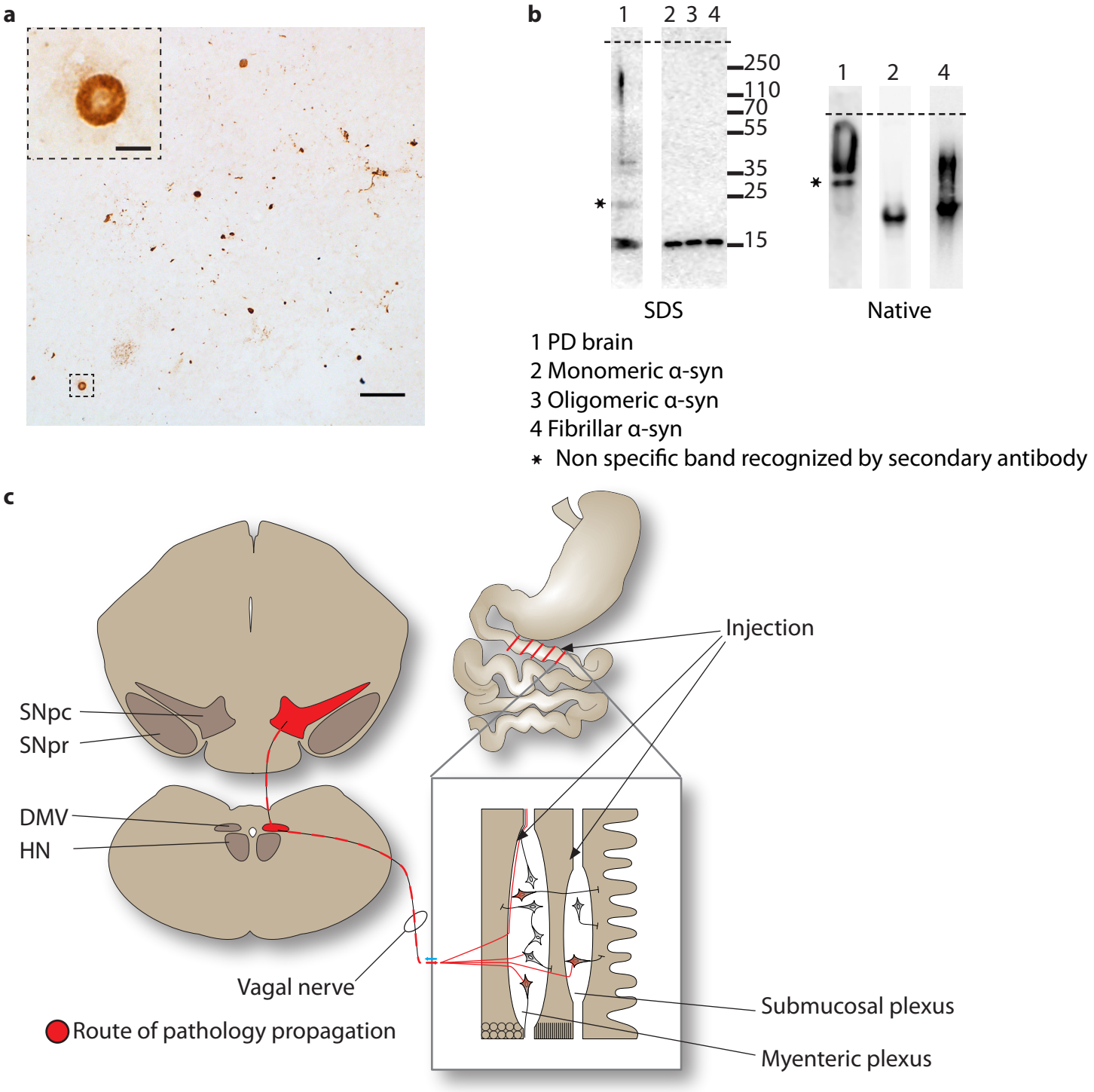
a
b
1 2 3 4
250
110
70
55
35
25
15
1 2 4
SDS
Native
1 PD brain
2 Monomeric α-syn
3 Oligomeric α-syn
4 Fibrillar α-syn
∗ Non specific band recognized by secondary antibody
c
Injection
SNpc
SNpr
DMV
HN
Vagal nerve
Route of pathology propagation
Submucosal plexus
Myenteric plexus
d 12h
BSA
PD Lysate
Fibrils
syn211
BSA
100 µm
50 µm

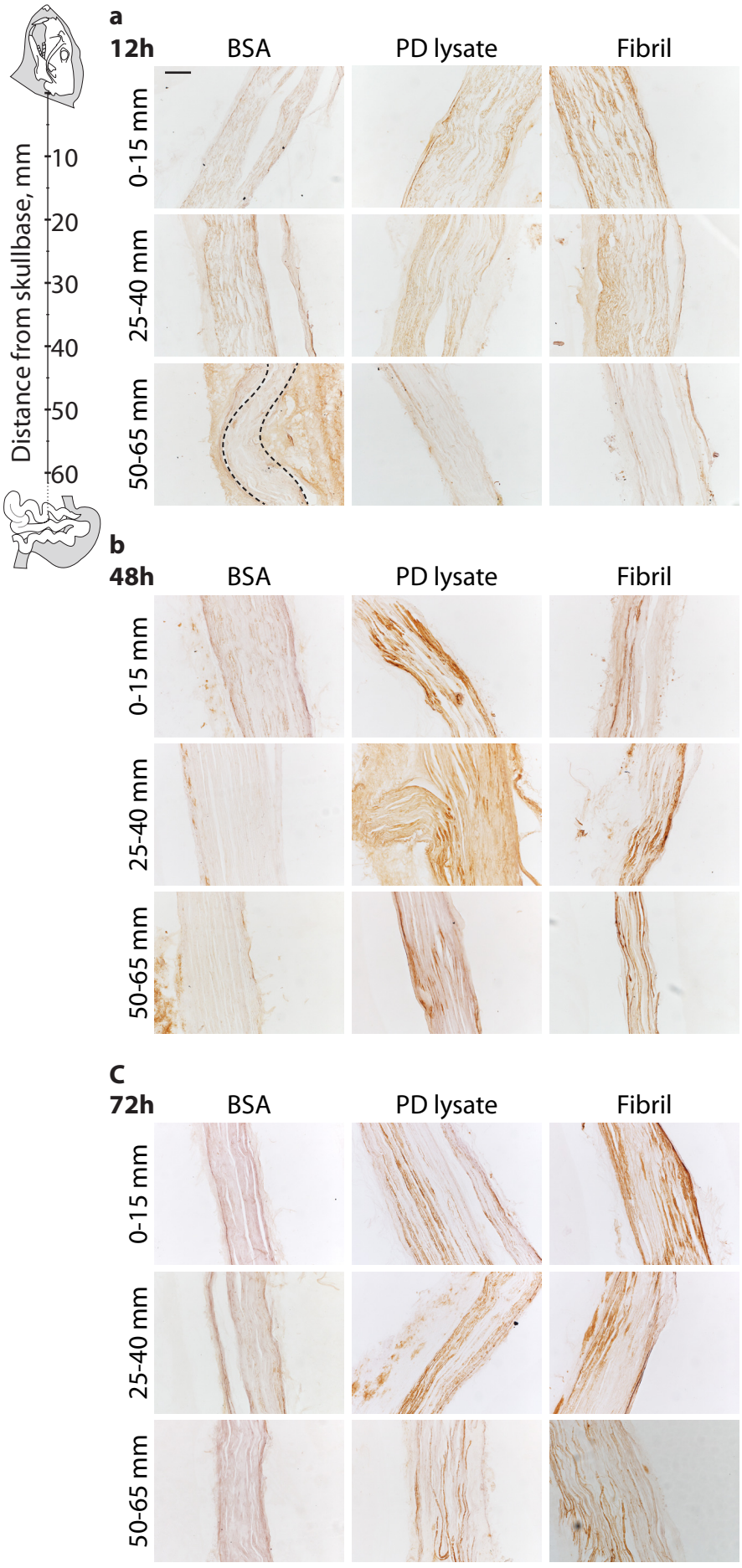
a
12h
BSA
PD lysate
Fibril
0-15 mm
25-40 mm
50-65 mm
Distance from skullbase, mm
10
20
30
40
50
60
b
48h
BSA
PD lysate
Fibril
0-15 mm
25-40 mm
50-65 mm
C
72h
BSA
PD lysate
Fibril
0-15 mm
25-40 mm
50-65 mm

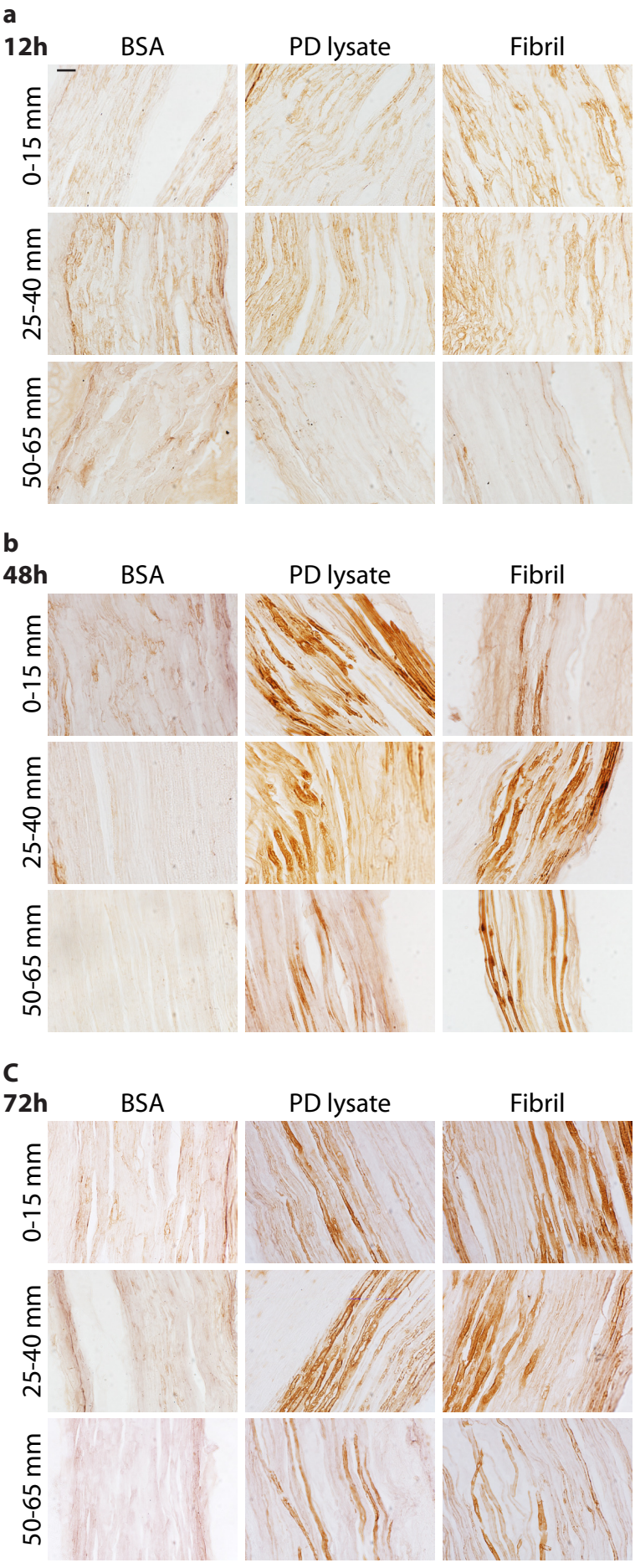
a
12h
BSA
PD lysate
Fibril
0-15 mm
25-40 mm
50-65 mm
b
48h
BSA
PD lysate
Fibril
0-15 mm
25-40 mm
50-65 mm
C
72h
BSA
PD lysate
Fibril
0-15 mm
25-40 mm
50-65 mm

a

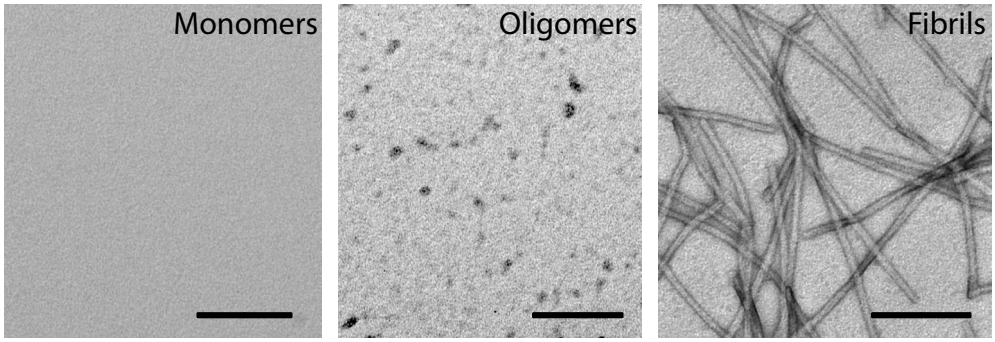
Monomers
Oligomers
Fibrils

b

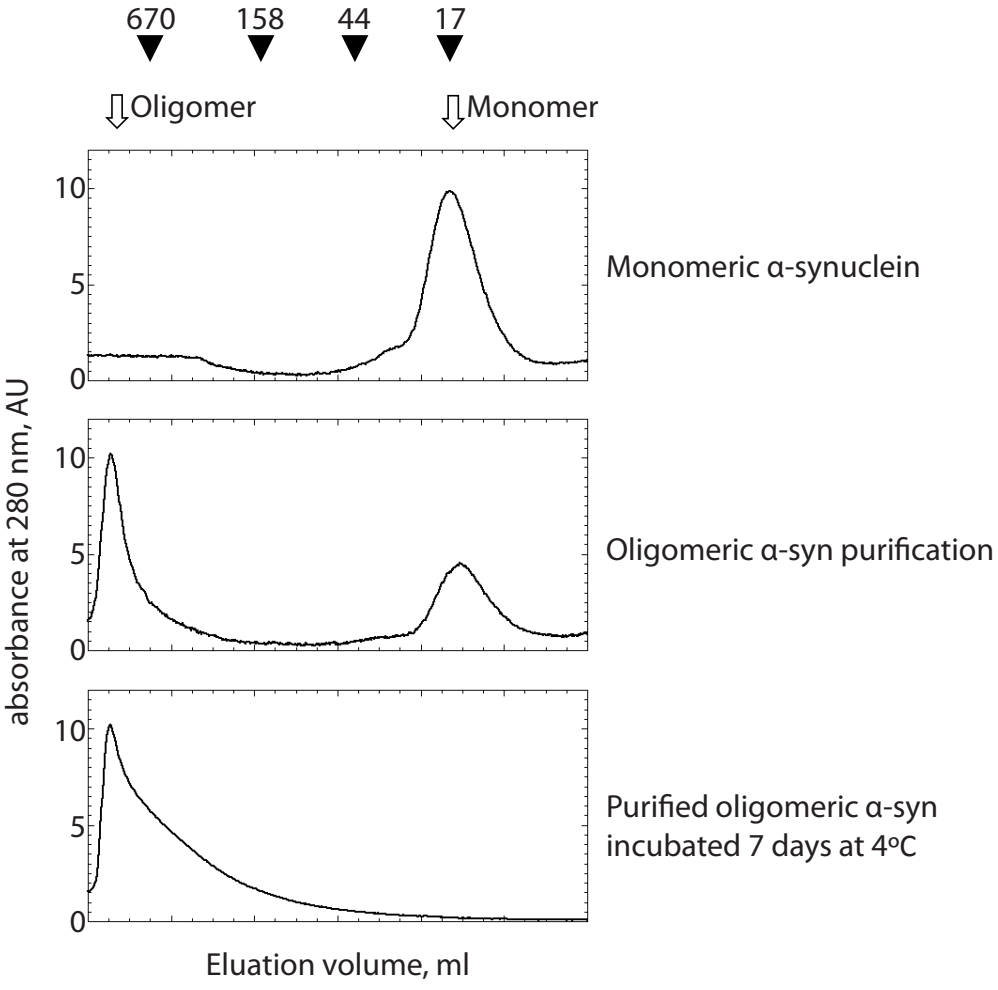
670
158
44
17
Oligomer
Monomer
10
5
0
absorbance at 280 nm, AU
Monomeric α-synuclein
Oligomeric α-syn purification
Purified oligomeric α-syn
incubated 7 days at 4°C
Eluation volume, ml

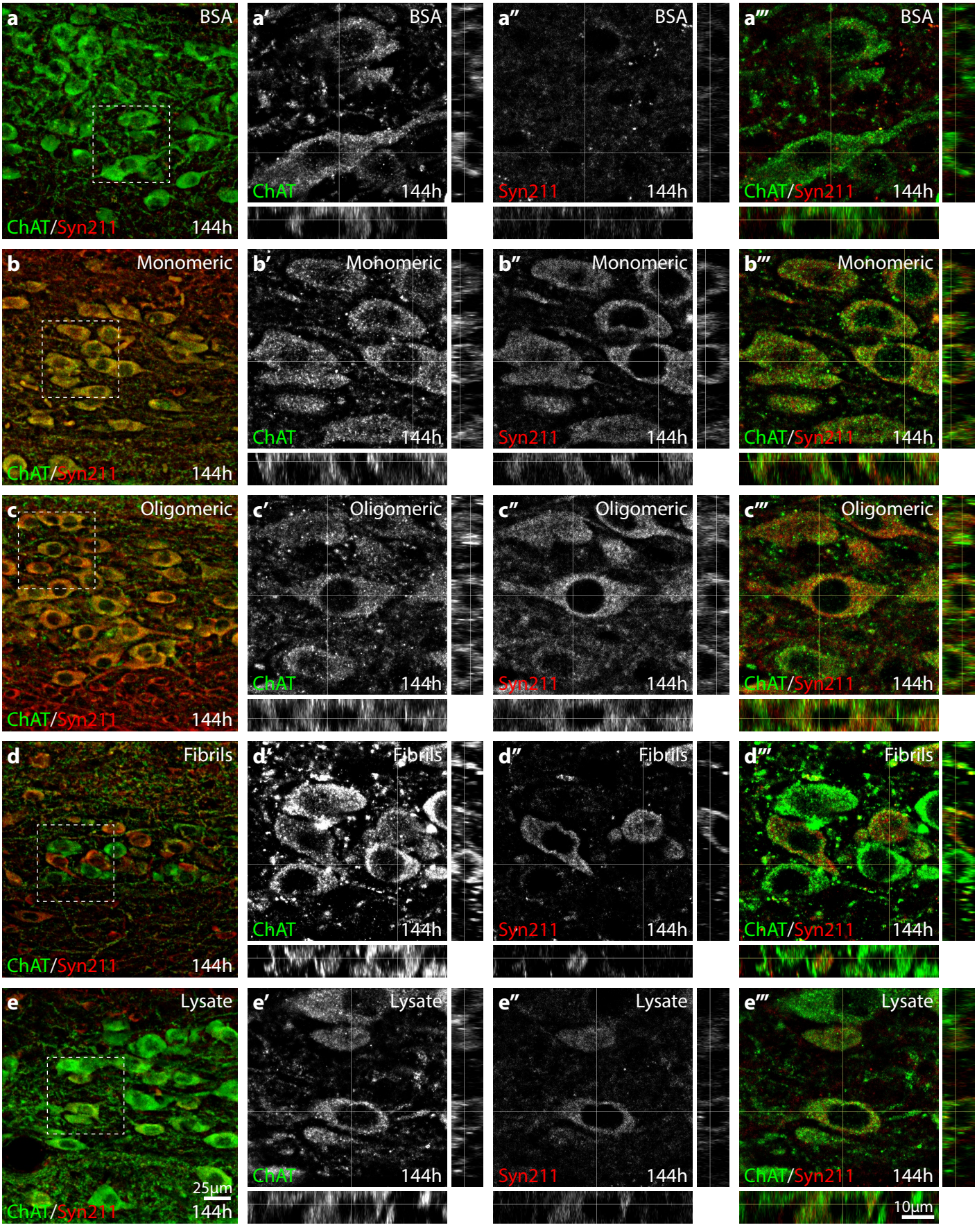
a
BSA
ChAT/Syn211
144h
a'
BSA
ChAT
144h
a''
BSA
Syn211
144h
a'''
BSA
ChAT/Syn211
144h
b
Monomeric
ChAT/Syn211
144h
b'
Monomeric
ChAT
144h
b''
Monomeric
Syn211
144h
b'''
Monomeric
ChAT/Syn211
144h
c
Oligomeric
ChAT/Syn211
144h
c'
Oligomeric
ChAT
144h
c''
Oligomeric
Syn211
144h
c'''
Oligomeric
ChAT/Syn211
144h
d
Fibrils
ChAT/Syn211
144h
d'
Fibrils
ChAT
144h
d''
Fibrils
Syn211
144h
d'''
Fibrils
ChAT/Syn211
144h
e
Lysate
25µm
ChAT/Syn211
144h
e'
Lysate
ChAT
144h
e''
Lysate
Syn211
144h
e'''
Lysate
ChAT/Syn211
144h
10µm

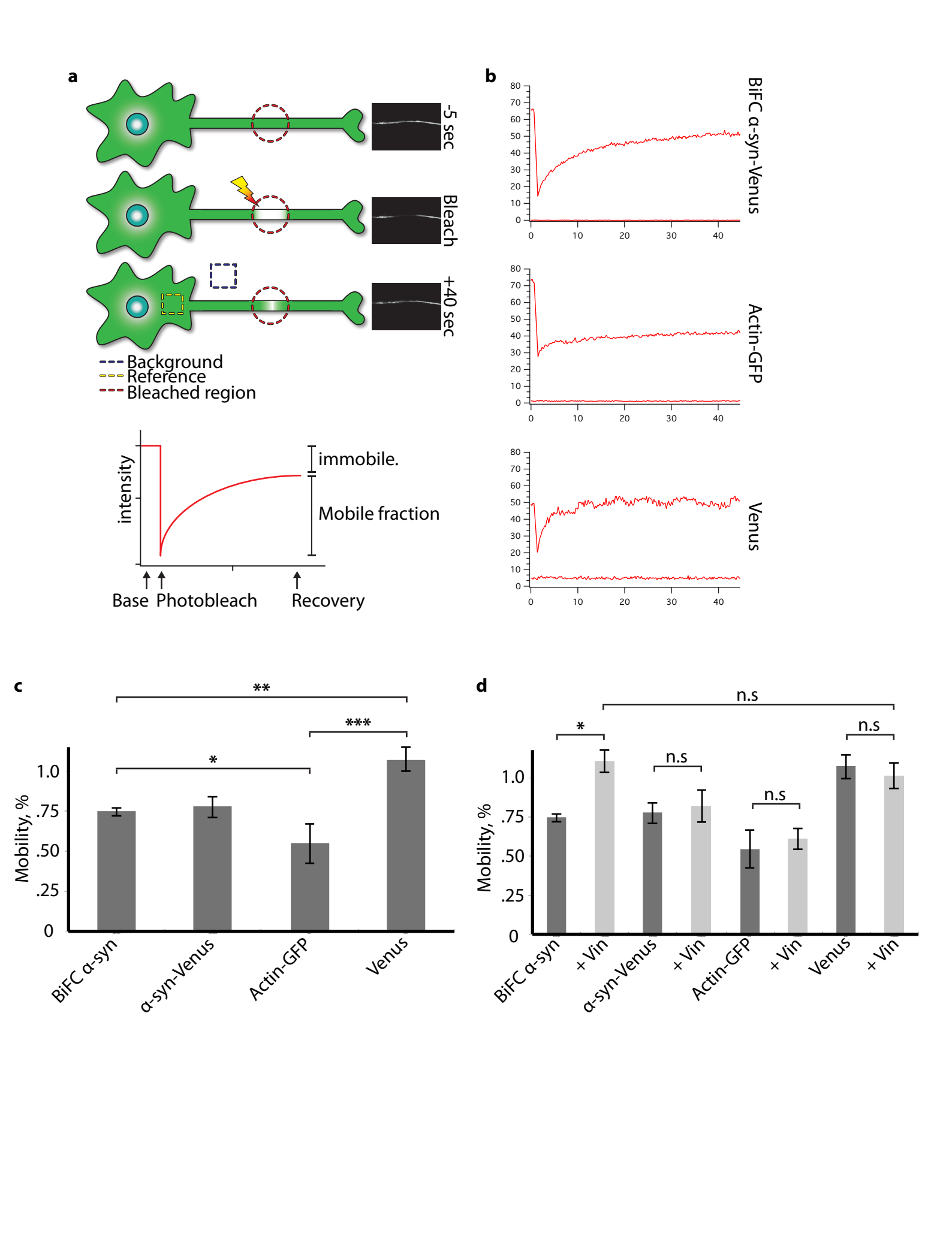
a
-5 sec
Bleach
+40 sec
Background
Reference
Bleached region
intensity
immobile.
Mobile fraction
Base
Photobleach
Recovery
b
BiFC α-syn-Venus
Actin-GFP
Venus
c
**
***
*
Mobility, %
1.0
.75
.50
.25
0
BiFC α-syn
α-syn-Venus
Actin-GFP
Venus
d
n.s
*
n.s
n.s
n.s
Mobility, %
1.0
.75
.50
.25
0
BiFC α-syn
+ Vin
α-syn-Venus
+ Vin
Actin-GFP
+ Vin
Venus
+ Vin

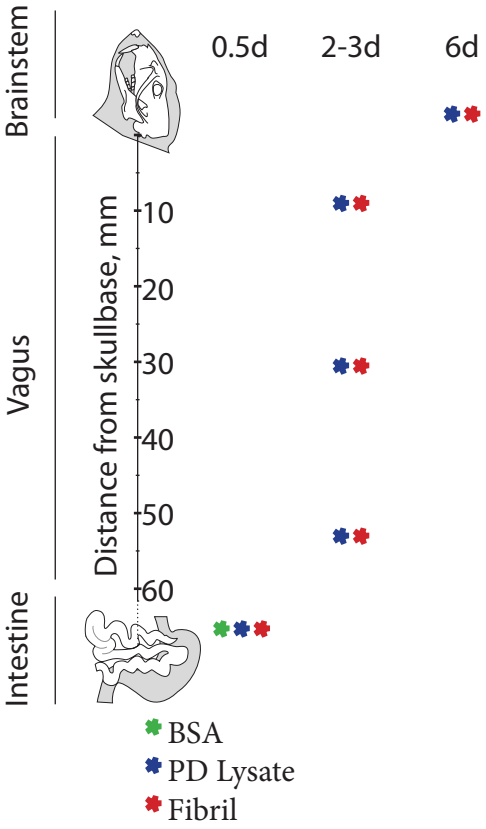
Brainstem
Vagus
Intestine
0.5d
2-3d
6d
Distance from skullbase, mm
10
20
30
40
50
60
BSA
PD Lysate
Fibril

Supplement information

Supplement Fig. 1. BSA in the vagal nerve. The actual levels of the segments of the vagal nerves are shown on the left of the images. Rats received injections of BSA (left), PD lysate (middle) or α-synuclein fibrils (right). The sections of vagal nerves were immunostained with an antibody against BSA. Twelve (a), 48 (b) and 72 (c) hours after the injection, no distinct BSA immunoreactivity was observed in nerve fibers of the vagal nerves at different time points, suggesting that BSA is not transported in the vagal nerve. Low power images scale bar 50 µm, and 20 µm in insets.

Supplement Fig. 2. Different α-synuclein forms specifically transported into the motor nucleus of the vagus. Imaging of α-synuclein-atto-550 after injection into the intestinal wall together with fluorogold, showing long-distance transport of human-α-synuclein to cell bodies of the DMV. Images of fluorogold (a-d) and human-α-synuclein conjugated to atto-550 (a'-d'). Animals injected with monomeric, oligomeric and fibrillar α-synuclein display numerous fluorescence punctae (a-a'', b-b'', c-c'', arrowheads). Brain lysate injected animals solely display signal for fluorogold (d-d''), but lack the distinct atto-550 label. Scale bar, 50 µm.

Supplement Fig. 3. α-synuclein forms specifically transported into the DMV, 24 hours after injection. The brain sections were immunostained with antibodies specific against human α-synuclein (Syn211, red, a-e, a''-d'', a'''-e''')) and ChAT (green, a-e, a'-d', a'''-e'''), the phenotypic markers of the DMV. BSA (a), Monomeric (b), oligomeric (c), fibrillar (d) α-

synuclein and PD patient brain lysate (e) were injected. No distinct human α-synuclein positive structures are found at this time point. Scale Bars, 25 µm in a-e, and 10 µm in a'''-e'''.

Supplement Fig. 4 Images of cell body axon-like protrusions in differentiated SH-SY5Y cells expressing complemented α-synuclein-Venus, actin-GFP or Venus alone. Series of images show fluorescently marked proteins before and after bleach and subsequent recovery signal during 40s.

Supplement Movie. Functional axonal transport visualized by active mitochondrial transport in synapse-like formation at end of neurite in RA differentiated SH-SY5Y cells. Images captured by confocal microscope and converted to movie in ImageJ.

Supplement Equations.

$$I_{frap-norm}(t) = \frac{I_{reference-pre}}{I_{reference}(t) - I_{bkgr}(t)} \times \frac{I_{frap}(t) - I_{bkgr}(t)}{I_{frap-pre}} \qquad (1)$$

Supplementary Equation (1). Background correction normalization

$$I_{decay}(t) = A_{decay} e^{(\tau_{decay})t} + y_{0-decay} \qquad (2)$$

Supplementary Equation (2). Correction for decay of fluorescence

$$Gap\ ratio = \frac{I_{reference-pre-estimated}}{I_{ref-pre-measured}} \qquad (3)$$

Supplementary Equation (3). For calculation of Gap ratio using reference region, enabling a more precise calculation of mobile / immobile fractions of the protein.

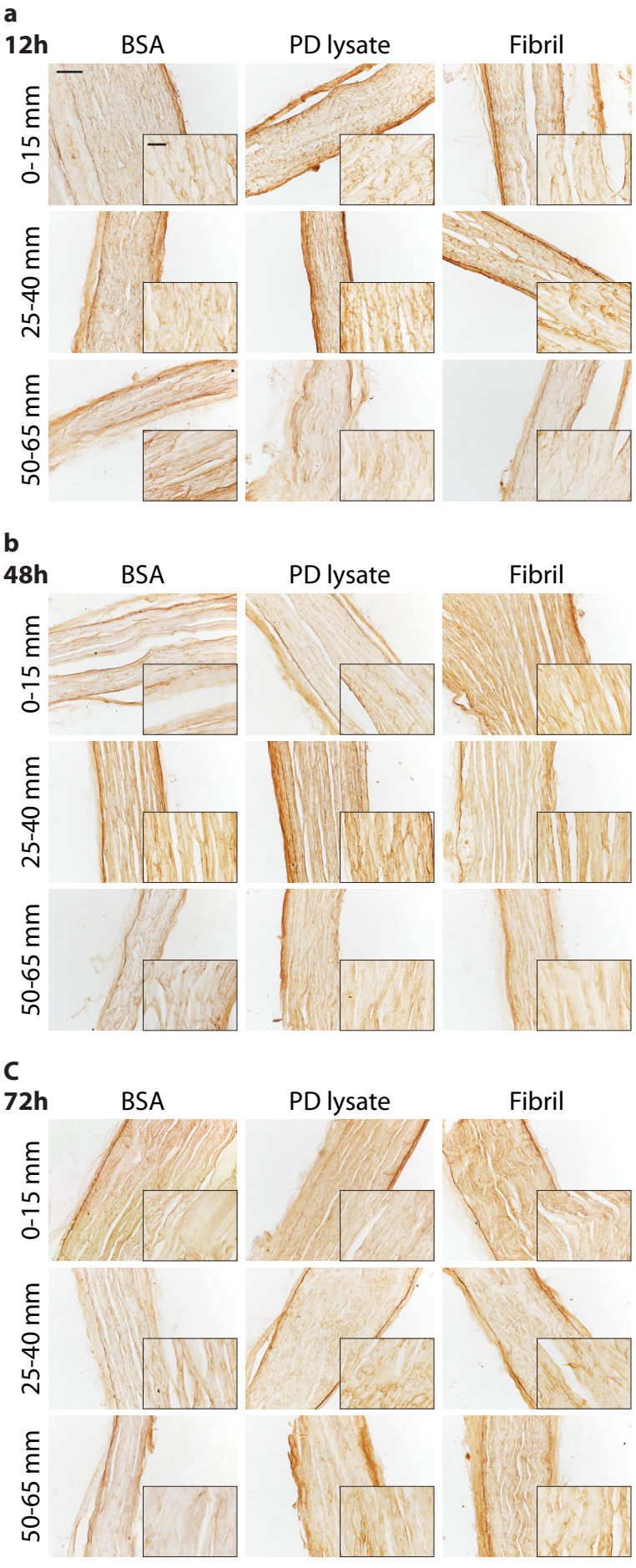
a
12h
BSA
PD lysate
Fibril
0-15 mm
25-40 mm
50-65 mm
b
48h
BSA
PD lysate
Fibril
0-15 mm
25-40 mm
50-65 mm
C
72h
BSA
PD lysate
Fibril
0-15 mm
25-40 mm
50-65 mm

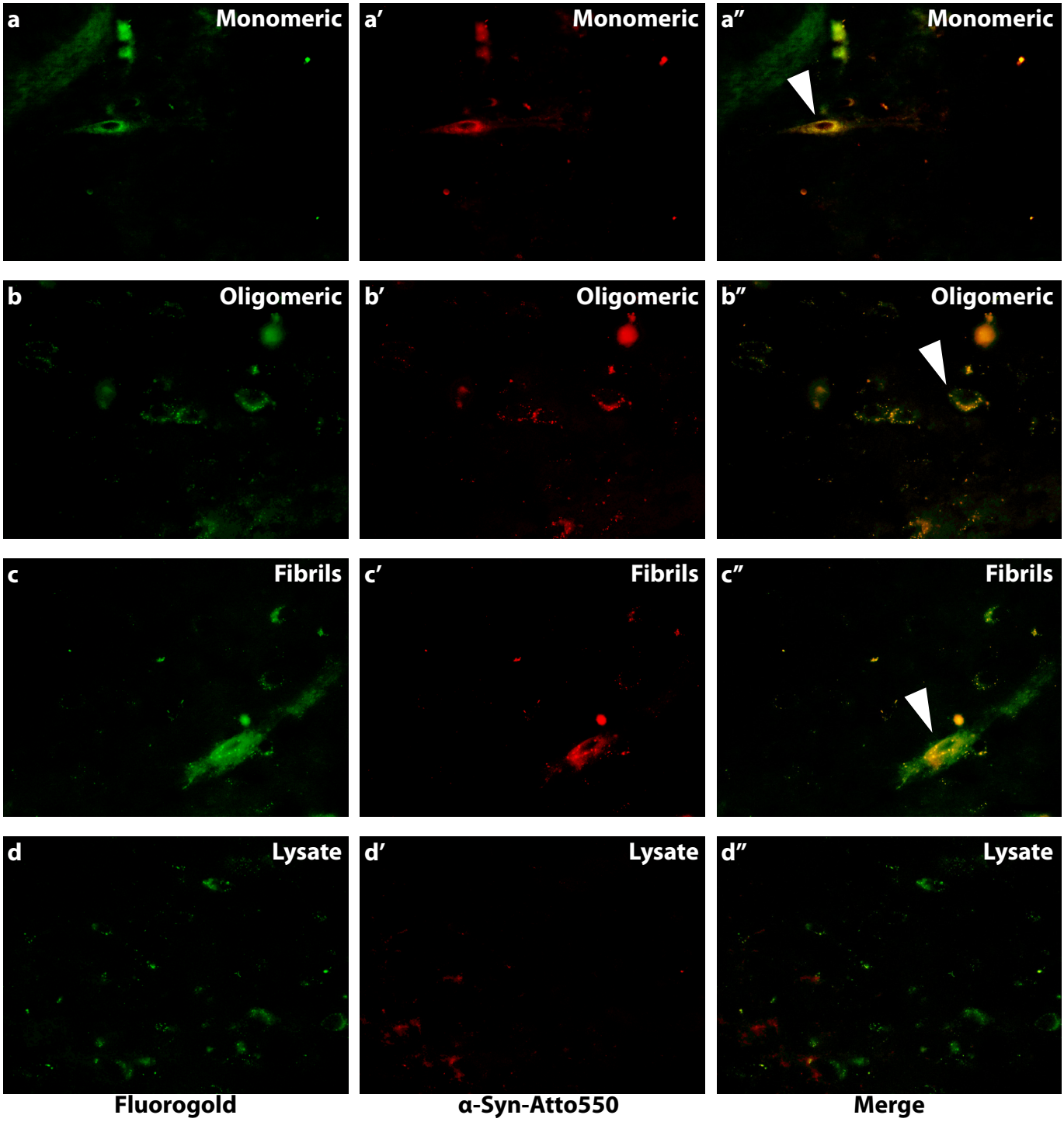
a
Monomeric
a′
Monomeric
a″
Monomeric
b
Oligomeric
b′
Oligomeric
b″
Oligomeric
c
Fibrils
c′
Fibrils
c″
Fibrils
d
Lysate
d′
Lysate
d″
Lysate
Fluorogold
α-Syn-Atto550
Merge

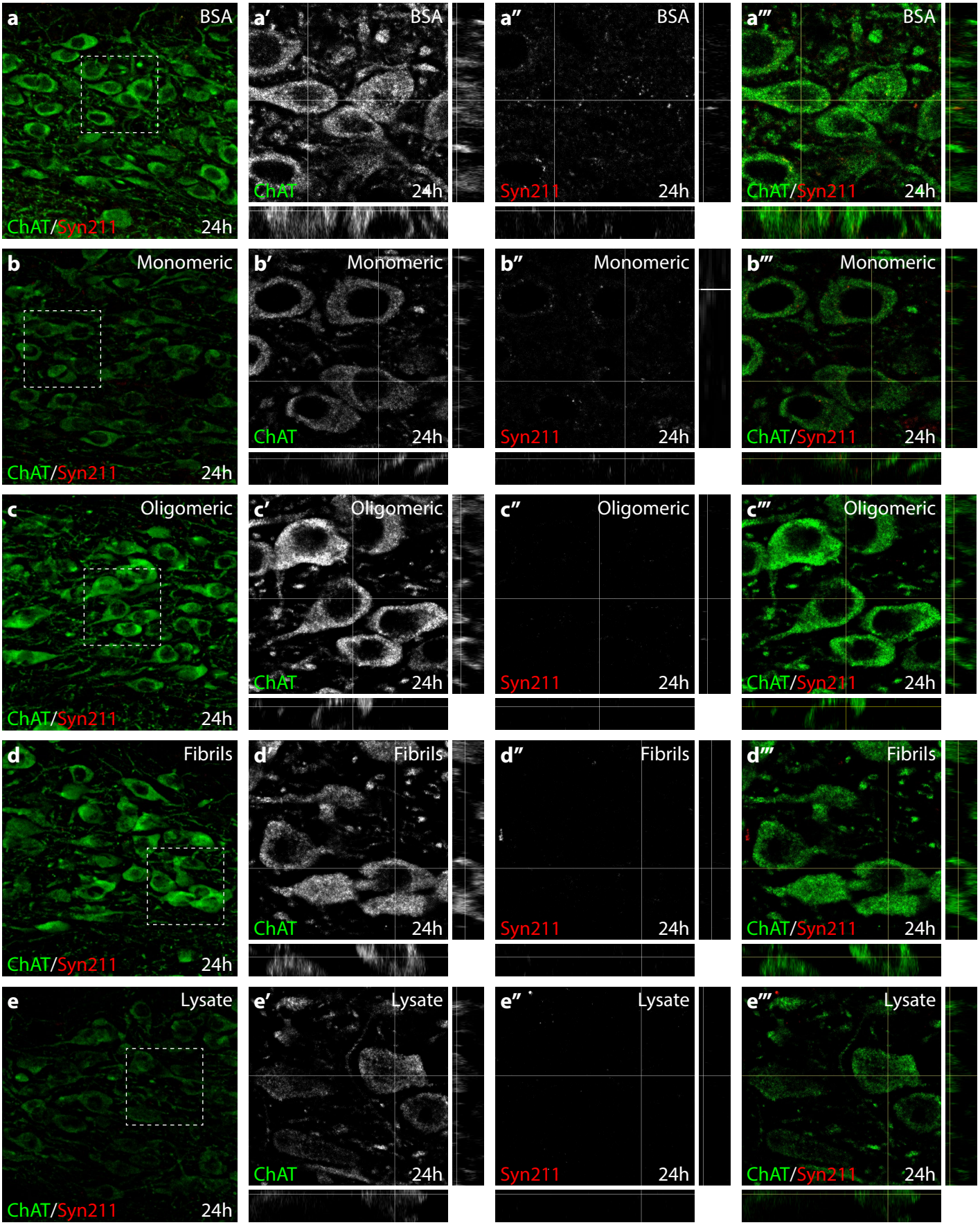
a
BSA
ChAT/Syn211
24h
a′
BSA
ChAT
24h
a″
BSA
Syn211
24h
a‴
BSA
ChAT/Syn211
24h
b
Monomeric
ChAT/Syn211
24h
b′
Monomeric
ChAT
24h
b″
Monomeric
Syn211
24h
b‴
Monomeric
ChAT/Syn211
24h
c
Oligomeric
ChAT/Syn211
24h
c′
Oligomeric
ChAT
24h
c″
Oligomeric
Syn211
24h
c‴
Oligomeric
ChAT/Syn211
24h
d
Fibrils
ChAT/Syn211
24h
d′
Fibrils
ChAT
24h
d″
Fibrils
Syn211
24h
d‴
Fibrils
ChAT/Syn211
24h
e
Lysate
ChAT/Syn211
24h
e′
Lysate
ChAT
24h
e″
Lysate
Syn211
24h
e‴
Lysate
ChAT/Syn211
24h

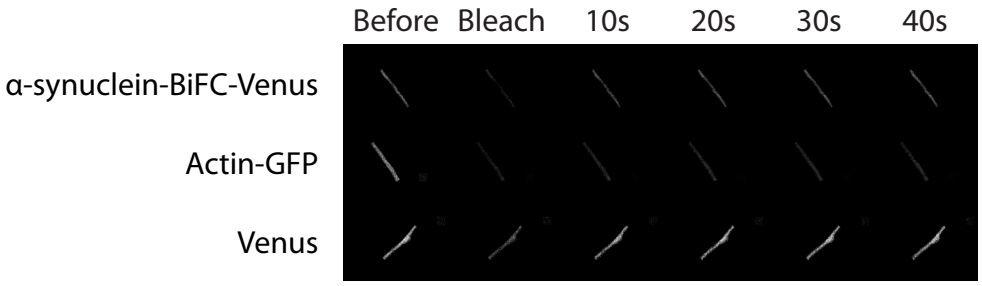
Before
Bleach
10s
20s
30s
40s
α-synuclein-BiFC-Venus
Actin-GFP
Venus